

ResearchSpace@Auckland

Version

This is the Accepted Manuscript version. This version is defined in the NISO recommended practice RP-8-2008 <http://www.niso.org/publications/rp/>

Suggested Reference

Swedlund, P.J., Holtkamp, H., Song, Y., & Daughney, C. J. (2014). Arsenate–Ferrihydrite Systems from Minutes to Months: A Macroscopic and IR Spectroscopic Study of an Elusive Equilibrium. *Environmental Science and Technology*, 48(5), 2759-2765. doi: 10.1021/es404742c

Copyright

Items in ResearchSpace are protected by copyright, with all rights reserved, unless otherwise indicated. Previously published items are made available in accordance with the copyright policy of the publisher.

This document is the Accepted Manuscript version of a Published Work that appeared in final form in *Environmental Science and Technology*, copyright © American Chemical Society after peer review and technical editing by the publisher. To access the final edited and published work see <http://doi.org/10.1021/es404742c>

<http://www.sherpa.ac.uk/romeo/issn/0013-936X/>

<https://researchspace.auckland.ac.nz/docs/uoa-docs/rights.htm>

1 The arsenate-ferrihydrite system from minutes to
2 months: A macroscopic and IR spectroscopic study
3 of an elusive equilibrium.

4

5 *Peter J. Swedlund^{1*}, Hannah Holtkamp¹, Yantao Song¹, Christopher J. Daughney²*

6 ¹School of Chemical Sciences, University of Auckland, Private Bag 92019, New Zealand

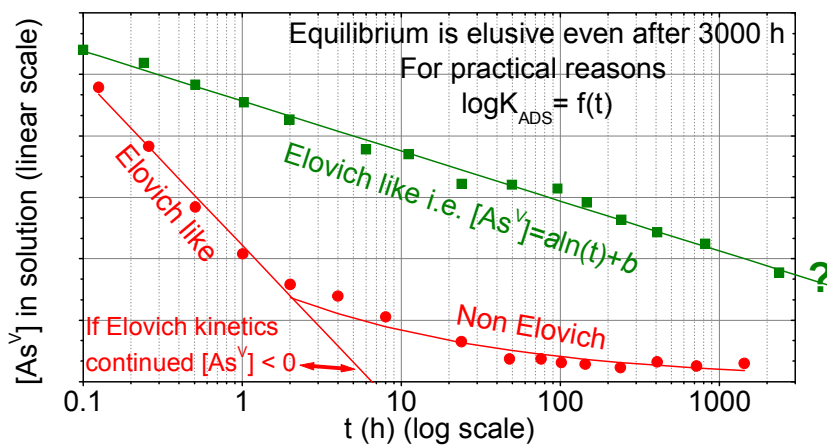
7 ²Institute of Geological and Nuclear Sciences, P.O. Box 30368, Lower Hutt, New Zealand

8

9

1 ABSTRACT: Sorption by ferrihydrite is an important control on As(V) concentrations in many
 2 oxic aquatic systems. There are significant discrepancies in reported sorption constants ($\log K_{As}$)
 3 which presents a problem for quantifying and understanding this important system. A review of
 4 reported ferrihydrite-As(V) sorption studies indicated a positive correlation between reaction
 5 time used in the experiments and the $\log K_{As}$ values derived from the data. In this paper we study
 6 the kinetics of As(V) sorption over ≈ 3000 h in nine systems with varying pH and As(V)/Fe.
 7 Ferrihydrite was stable in all systems containing As(V) and the [As(V)] in solution decreased
 8 linearly as a function of $\log(t)$ (termed Elovich kinetics) over the full 3000 h in most systems. A
 9 stable [As(V)] was only observed in systems with low As(V)/Fe and low pH. Apparent As(V)
 10 sorption constants were derived from the data at specific times intervals using the Diffuse Layer
 11 Model and equations describing $\log K_{As}$ values as a function of time provide a way to describe
 12 this elusive equilibrium. IR spectra support the hypothesis that slow inter-particle diffusion is
 13 responsible for the slow approach to equilibrium. This work resolves previous discrepancies in
 14 previous studies of As(V)-ferrihydrite and provides equations to allow for system appropriate
 15 $\log K_{As}$ values to be used.

16 **TOC\Abstract Graphic**



17

1 Introduction

2 Uncertainty remains in the geochemical controls of arsenic solubility despite the fact that
3 arsenic in drinking water adversely impacts millions of people globally.¹ In oxic systems the
4 principal mechanisms controlling solution AsO_4^{-3} concentrations, termed As_{sol} , are reactions on
5 the surfaces of iron oxyhydroxides which under most circumstances have been shown to be
6 sorption reactions.² Ferrihydrite is an important AsO_4^{-3} sorbent however there is considerable
7 variation in reported equilibrium constants for AsO_4^{-3} sorption by ferrihydrite³ This paper
8 demonstrates how kinetic factors contribute to discrepancies in modelling the ferrihydrite- AsO_4^{-3}
9 system and presents an explanation for this and an approach for modeling the system on a
10 variable time scale.

11 Surface complexation models can be powerful tools to decipher and quantify the complex
12 interactions affecting sorption. Using a small number of adjustable parameters the Diffuse Layer
13 Model (DLM) is able to describe the macroscopic features of the ferrihydrite sorption of anions
14 such as the effects of pH,⁴ ionic strength (I),⁵ surface coverage (Γ) and competing ions.⁶ The
15 DLM is used in this work for this reason and to allow comparison with the large number of
16 previous studies using the DLM for AsO_4^{-3} -ferrihydrite systems. The DLM derives its utility for
17 macroscopic predictions by separating out chemical and electrostatic contributions to sorption
18 reactions but the model does not provide information relating to surface complex structures and
19 this dichotomy has been discussed.⁷ Debate persists on surface complex structure and model
20 approaches^{8, 9} and all the data from this study are presented in the Supplementary Information
21 section to support alternative model approaches.

22 In the DLM AsO_4^{-3} sorption is a ligand exchange reaction with a hydroxide group on a
23 ferrihydrite surface site ($\equiv\text{FeOH}$) forming surface complexes of different degrees of protonation.

1 The equilibrium expressions are given in Table 1 with the means and ranges of DLM sorption
2 constants ($\log K$'s) compiled from available literature data by Gustafsson and Bhattacharya.³
3 These $\log K$ values have a high level of variability which creates significant uncertainty in
4 predicted AsO_4^{-3} sorption and it is desirable to resolve this. In general anomalously large $\log K_{\text{As}}$
5 values were derived from the data from Swedlund and Webster⁶ that was obtained with an
6 anomalously long reaction time of 200 h. Note that Gustafsson and Bhattacharya³ mistakenly
7 state the reaction time used for all Swedlund and Webster⁶ data was 24 h. Regression analysis of
8 the $\log K_{\text{As}}$ values from Gustafsson and Bhattacharya³ versus the \log_{10} of the reaction time have
9 positive slopes but these have a high uncertainty (Table 1) which is partly a reflection of the fact
10 that the kinetics of sorption depends greatly on the $\text{AsO}_4^{-3}/\text{Fe}$ ratio and this is discussed further in
11 the modeling section.

12 In this work we quantify the significant contribution of kinetic factors to the variance in these
13 reported ferrihydrite- AsO_4^{-3} $\log K$'s. Numerous studies have shown that the concept of
14 equilibrium is not directly applicable to ion sorption on iron oxides. For example in ferrihydrite
15 sorption experiments Scheinost et al¹⁰ observed that Cu^{+2} and Pb^{+2} solution concentrations
16 decreased linearly as a function of $\log(\text{time})$ for 10^3 h, which was the duration of the experiment.
17 Zhang and Stanforth¹¹ found that the adsorption kinetics of AsO_4^{-3} on goethite were generally
18 well described by the Elovich Equation in which Γ has a linear dependence on $\log(t)$ and this has
19 been variously attributed to inter- or intra-particle diffusion or site heterogeneity.^{12, 13} Aquatic
20 systems of interest to public health such as water treatment systems or aquifers involve time
21 scales ranging from minutes to decades and a model with a single set of equilibrium constants
22 cannot be applicable to AsO_4^{-3} distribution across all of these systems.

23 In this paper we follow AsO_4^{-3} adsorption onto ferrihydrite over 3600 h in batch systems with a
24 range of total AsO_4^{-3} concentrations (termed As_{tot}) and pH. Because ferrihydrite is metastable,

1 solid samples were freeze dried and analyzed with infrared and Raman spectroscopy to test the
2 stability of the ferrihydrite phase. The data were used to derive new time-dependent $\log K_{As}$
3 which account for the change in $A_{S_{sol}}$ with time. The system was also probed with *in situ* and *ex*
4 *situ* attenuated total reflectance infrared (ATRIR) spectroscopy in separate experiments to shed
5 light on the processes involved.

6
7
8

9 **Method**

10 All experiments were conducted at room temperature (21°C) using water with resistivity of
11 18.2 MΩ cm which was acidified (pH < 4) and sparged with N₂ for 1 hour to remove CO₂. All
12 solutions were kept under N₂. The pH was adjusted with HNO₃ or with NaOH. To minimise the
13 presence of carbonate NaOH solutions were prepared weekly from 1:1 (w/w) NaOH:H₂O.
14 Ferrihydrite was synthesized 12-18 h before sorption experiments by rapidly raising the pH of a
15 Fe(NO₃)₃ solution from 2 to 8 and the phase present was confirmed by XRD.⁶

16 Arsenate sorption by \approx 1mM ferrihydrite (i.e. \approx 0.089 g L⁻¹) was measured as a function of time
17 in batch systems having $A_{S_{tot}}$ of \approx 50, 100, or 200 μM and 0.06 M NaNO₃. At each $A_{S_{tot}}$ sorption
18 was measured at pH 6, 8, and 10 so that in all 9 systems were studied. Polycarbonate containers
19 were used and previous experiments have shown that at these concentrations of $A_{S_{tot}}$ sorption to
20 container walls is negligible compared to sorption by iron oxides.⁶ Samples were taken at \approx 0.13,
21 0.25, 0.5, and 1 h and then at increasing time intervals over 3,000 h (125 days). The suspensions
22 were stirred rapidly during sampling so that there was no change in the solids concentration over
23 time. Suspensions were kept on a magnetic stirrer for the first 8 h to allow for continuous pH

1 monitoring and manual correction but after 8 h the pH drift was small and samples were placed
2 on an end-over-end mixer at a rate of ≈ 5 rpm and pH drifts (typically < 0.1 pH unit) were
3 manually corrected daily at least one hour prior to sampling. Samples were centrifuged (4,000
4 rpm, 5 minutes), the supernatant was filtered (0.2 μm cellulose acetate membrane) and the solids
5 collected, briefly rinsed once with ≈ 0.06 M KCl and freeze dried for IR and Raman analysis to
6 test ferrihydrite phase stability. A 10 mL unfiltered aliquot of each suspension was digested with
7 ≈ 1 drop of 35 % HCl to determine the total Fe and As concentrations.

8 *Aqueous Analysis*

9 The suspension pH was measured using a London Scientific Instruments annular ring
10 electrode. The As_{sol} was determined using either the molybdenum blue method¹⁴ or ICP-MS.
11 The molybdenum blue method LOD was 0.45 μM and samples with lower As_{sol} were analysed by
12 ICP-MS which had a LOD of 0.067 μM . Selected samples with $1 < \text{As}_{\text{sol}} < 200$ μM were
13 analysed by both methods and a linear regression of this data had a slope of 1.0037 with R^2
14 0.993. All HCl digests of unfiltered suspensions were analysed by ICP-MS.

15 *Vibrational spectroscopy*

16 The freeze-dried solid samples collected during the batch sorption experiments were
17 characterized by Raman and IR to check for development of crystalline phases. Raman spectra
18 were measured using a 785 nm laser on a Renishaw Raman System 1000 spectrometer. The IR
19 spectra were measured using a single bounce 45° diamond ATR crystal on a Nicolet[®] 8700
20 Spectrometer. Freeze dried reference samples of ferrihydrite, goethite, lepidocrocite and
21 hematite were prepared following the method of Schwertmann and Cornell¹⁵ and phases
22 confirmed by X-ray diffraction. In addition two types of ATRIR experiments probed the
23 interfacial AsO_4^{3-} . *In situ* ATRIR spectra were recorded over time as AsO_4^{3-} reacted with

1 ferrihydrite that had been deposited by drying on a single bounce 45° diamond ATR crystal as
2 previously described.¹⁶ In addition ATRIR spectra were measured of ferrihydrite pastes that
3 were obtained by centrifuging (4,000 rpm) suspensions to which AsO_4^{-3} was added.

4 *Modelling*

5 The adsorption data were modeled using the DLM and ferrihydrite parameters of Dzombak and
6 Morel.¹⁷ This includes a single sorption site type with a site density of $0.2 \text{ mol (mol Fe)}^{-1}$, a
7 surface area of $600 \text{ m}^2\text{g}^{-1}$, a ferrihydrite M_w of 89 g mol^{-1} and surface site pK_A 's of 7.29 and 8.93.
8 Adsorption constants were determined at each sampling time from 0.125 h to ≈ 3000 h using
9 FITEQL4.¹⁸ At each time interval a set of 9 data points are available to optimize the $\log K_{As}$'s.
10 Each data point consists of a solids concentration in gL^{-1} (i.e. $89 \text{ g mol}^{-1} \times [\text{Fe}^{+3}]$ in M), the
11 number of surface sites (i.e. $0.2 \times [\text{Fe}^{+3}]$ in M), the As_{tot} , the As_{sol} and the -pH (i.e. $\log(\text{H}^+)$).
12 Equations describing the decrease in As_{sol} over time allow for any time interval to be chosen. All
13 the values can simply be input as serial data although the solids concentration is usually input as
14 a single value for a series of data. The solids concentration is combined with the surface area
15 (m^2g^{-1}) to give the number of m^2 of surface present so that a surface charge can be calculated. In
16 our case the solids concentration varied slightly between different systems and it was desirable to
17 be able to use the appropriate value for each data point. Methods to use FITEQL with different
18 [solids] have been reported¹⁹ but a little known feature in FITEQL is that solids concentrations
19 can be input as serial data using component number 160 which is formally the surface potential
20 component.²⁰ The measured As_{sol} was input as a “dummy component”.

21 The input uncertainties in measured values were based on the method of Dzombak and
22 Morel¹⁷. Calculations were done at the average ionic strength of 0.064 M using activity
23 coefficients for solution species calculated from the Davis equation and all reported $\log K$'s are
24 reported at an ionic strength of 0 M. Initial guesses for the $\log K_{Asx}$ were taken from

1 VMINTEQ.²¹ The goodness of fit is judged by the weighted sum of squares divided by the
2 degrees of freedom (WSOS/DF) with values between 0.1 and 20 are considered a good fit.^{6, 17}
3 To check the validity of the FITEQL4 input files speciation was compared with that predicted by
4 VMINTEQ and was identical. An example of a text input and the screen shots from the FITEQL
5 Preprocessor are shown in the Supplementary Information section.

6 **Results and Discussion**

7 *Ferrihydrite phase stability*

8 Before considering the kinetic data it is necessary to assess the stability of the ferrihydrite as
9 changes in iron oxide phase will affect $A_{S_{sol}}$. The Raman and IR spectra of the freeze dried
10 solids (Figures SI1 and SI2) collected over the course of the kinetic experiments had no
11 discernible hematite, goethite or lepidocrocite bands. In addition the broad feature at $\approx 800\text{ cm}^{-1}$
12 shows the presence of AsO_4^{-3} on the ferrihydrite surface while the absence of IR bands at ≈ 1350
13 and 1470 cm^{-1} demonstrates the absence of carbonate on the ferrihydrite surface. Ferrihydrite is
14 only a meta-stable phase and over time converts to more stable iron oxides, including goethite
15 and hematite. In previous experiments with pure ferrihydrite kept in suspension at pH 10 we
16 have observed large goethite IR bands after 10 days.⁵ Goethite forms from ferrihydrite via Fe^{3+}
17 dissolution and reprecipitation and Das *et al*²² found that the adsorbed arsenate produces stable
18 surface complexes that prevents Fe^{+3} dissolution and inhibits the transformation into goethite or
19 hematite. The Raman and IR spectra from the current study show that the AsO_4^{-3} has stabilized
20 the ferrihydrite against transformation to goethite and we can state that the data in this work
21 represent the reaction of AsO_4^{-3} with ferrihydrite over time with no confounding effects due to
22 ferrihydrite phase transformations.

1 *Kinetics of arsenate adsorption*

2 The decrease in $A_{S_{sol}}$ over time in systems with $A_{S_{tot}} \approx 200 \mu\text{M}$ is presented in Figure 1 and
3 Table SI1. If data for the first 150 h are plotted with a linear time scale then AsO_4^{-3} sorption
4 shows the typical “two-stage” kinetics described in many studies with a rapid sorption step after
5 which sorption continues at a slower pace. With a logarithmic time scale data over the whole
6 course of the experiment ($\approx 3,000$ h) show a linear decrease in $A_{S_{sol}}$ as a function of $\log(t)$ at each
7 pH. As the pH of the suspension is decreased from pH 10 to pH 6 there is a corresponding
8 decrease in $A_{S_{sol}}$ and an increase in slope of the $A_{S_{sol}}$ vs $\log(t)$ line. This behavior is very similar
9 to that previously reported for cation sorption by ferrihydrite such as Scheinost *et al*¹⁰ who
10 explained the slow adsorption stage as being due to diffusion toward surface sites buried in the
11 interior of ferrihydrite aggregates. Fuller *et al*²³ also made a similar observation for AsO_4^{-3} and
12 ferrihydrite over ≈ 200 h and reached a similar explanation for the phenomenon. Figure 1 also
13 shows the predicted $A_{S_{sol}}$ for each system using the sorption constants from both Gustafsson
14 (derived from data with $t = 1$ to 200 h) and Swedlund and Webster which were derived from data
15 with $t = 24$ to 200 h⁶. The Gustafsson model agrees with the data from this work at $t \approx 2 - 10$ h
16 while the Swedlund and Webster model agrees with the data from this work at $t \approx 100 - 2000$ h.
17 The data from this work is evidently reasonably consistent with both these previous studies.

18

19 [Fig 1 about here]

20

21 For systems with $A_{S_{tot}}$ of $\approx 100 \mu\text{M}$ (Figure 2 and Table SI2) the $A_{S_{sol}}$ decreases linearly with
22 $\log(t)$ over the $\approx 2,500$ h course of the experiment at pH 10 and 8. However at pH 6 this is only
23 true for the first 10 h after which time $A_{S_{sol}}$ decreases asymptotically over $\log(t)$. This is a
24 physical necessity because the $A_{S_{sol}}$ would become negative beyond 18 h if the Elovich behavior

1 was extrapolated. In fact the $A_{S_{sol}}$ would become negative at some time for any system if it
2 continued to decrease linearly vs $\log(t)$ and in the system with pH 6 and $100 \mu\text{M } A_{S_{tot}}$ this occurs
3 within the time frame of the experiment. After ≈ 10 hours the decrease is more appropriately
4 described by a power function rather than a logarithmic function and the equations used to
5 describe all $A_{S_{sol}}$ vs time data are given in the figure. We do not attempt to infer some
6 mechanistic model from the change in function but use these functions to interpolate the $A_{S_{sol}}$ so
7 that we may calculate $\log K_{As}$ values at any time interval. The data at pH 6 and 8 agree with the
8 Gustafsson model at $t \approx 6$ h and with the Swedlund and Webster model at $t \approx 1000$ h. In
9 comparison the data for the system at pH 10 are all a bit below the Gustafsson model and agrees
10 with the Swedlund and Webster model at $t = 1$ h.

11 [Fig 2]

12 For systems with $A_{S_{tot}}$ of $\approx 50 \mu\text{M}$ (Figure 3 and Table SI3) the linear decrease in $A_{S_{sol}}$ vs $\log(t)$
13 is only evident for the first 8 h at pH 10 and the first 2 h at pH 8. At pH 6 after just 7.5 minutes
14 99.4 % of the $A_{S_{tot}}$ has been adsorbed and from 1 to 1000 h the $A_{S_{sol}}$ decrease is minimal, from \approx
15 0.1 to $0.08 \mu\text{M}$. The decrease over the first hour is best described by a power function and the
16 very slight decrease in $A_{S_{sol}}$ after 1 h is described by a log function with a slope of just -0.013.
17 The experiments with $\approx 50 \mu\text{M } A_{S_{tot}}$ and pH 6 and 8 were the only two systems where some sort
18 of $A_{S_{sol}}$ stability was achieved with no clear decrease in $A_{S_{sol}}$ after 20 or 100 h at pH 6 or 8
19 respectively. It is also noteworthy that there is no increase in $A_{S_{sol}}$ over time under any
20 conditions. In experiments where ferrihydrite was aged for up to 144 h prior to AsO_4^{-3} addition
21 the amount of AsO_4^{-3} sorption decreased the longer the ferrihydrite was aged and this was
22 attributed to the number of surface sites decreasing due to either crystallite growth or ongoing
23 coagulation as ferrihydrite aged.²³ In light of this result the absence of any increase in $A_{S_{sol}}$ over

1 time in the current study suggests that the presence of AsO_4^{-3} stabilizes the ferrihydrite not only
2 against phase transformation but also against processes which decrease surface site
3 concentrations over time.

4 At pH 10 the data agree with the Gustafsson model and the Swedlund and Webster model at \approx
5 0.5 and 1 h respectively while at pH 8 this occurs at $t \approx 2$ and 40 h. After 1 h at pH 6 the As_{sol}
6 was $\approx 0.1 \mu\text{M}$ while the models were 2 nM (Gustafsson) and 0.4 nM (Swedlund and Webster).
7 This is the most significant discrepancy between the data and the models (considering As_{sol} on a
8 logarithmic scale) and may indicate that some other process is occurring in these systems with
9 very low As_{sol} . If one considers sorbed As on any scale or considers As_{sol} on a linear scale the
10 difference is not significant. This has an impact on how one configures the FITEQL file and is
11 discussed below.

12 [Fig 3]

13 *The Log K_{As} 's over time*

14 Values for the $\log K_{\text{As}1}$ to $\log K_{\text{As}4}$ were optimized from the data at each time interval. Because
15 the data at pH 6 with $\approx 50 \mu\text{M}$ As_{tot} were not well described by the model, these data were
16 excluded in the parameter optimization process so at each time point there are eight data points.
17 Also note that Ali and Dzombak⁴ removed data points that corresponded to greater than or equal
18 to 85% sorption with the justification that FITEQL weights these data points too heavily which
19 produces biased log K values. All four $\log K_{\text{As}}$'s values could be optimized from the data
20 provided at each time interval and the optimized $\log K_{\text{As}}$'s as a function of time are presented in
21 Figure 4 and Table 2. The WSOS/DF all lay between 1.4 and 2.03 which demonstrates that the
22 data are well described by the model system and that the data also reasonably constrain the
23 $\log K_{\text{As}}$ values.

1 There is a clear linear increase for $\log K_{As1}$ to $\log K_{As3}$ as a function of $\log(t)$ although $\log K_{As4}$
2 appears to start to plateau after ≈ 10 h. In general, the slope of the line increases as the charge on
3 the surface species decreases and this was also observed in Table 1. This derives from the effect
4 of surface coverage on the modeled surface speciation. For simple electrostatic reasons a higher
5 AsO_4^{-3} surface coverage will in general favor the modeled species with a lower charge. For
6 example with 1 mM ferrihydrite the $\equiv FeOHAsO_4^{-3}$ species pH between 4 and 12 accounts for 62
7 % or 15 % of the sorbed AsO_4^{-3} with 1 μM As_{tot} or 100 μM As_{tot} respectively (Figure SI4). From
8 Figure SI4 it is clear that data with a lower $As_{tot}/[ferrihydrite]$ more tightly constrain $\log K_{As4}$
9 while data with higher $As_{tot}/[ferrihydrite]$ will more tightly constrain $\log K_{As1}$. Similarly σ_1
10 and σ_4 change systematically with Γ in Table 2. Data with lower $As_{tot}/[ferrihydrite]$ approach
11 equilibrium As_{sol} more rapidly thus the value of $\log K_{As4}$ changes less with time than $\log K_{As1}$.

12 *IR Spectroscopy of AsO_4^{-3} on ferrihydrite*

13 The As-O stretching region of the *in situ* ATR-IR spectra recorded over time as 200 μM AsO_4^{-3}
14 at pH 8.0 in 0.06 M NaCl reacted on a ferrihydrite film deposited on a diamond ATR crystal are
15 shown in Figure 5a. The area of this feature increased linearly as a function of $\log(\text{time})$ but the
16 spectra are shown with absorbance normalized to emphasize the fairly subtle change in their
17 shape over time. All spectra have a broad maximum at ≈ 810 cm^{-1} with a shoulder at ≈ 870 cm^{-1} .
18 Over time as Γ increases the shoulder becomes more prominent and shifts from 861 to 876 cm^{-1}
19 as is particularly evident in the 2nd derivatives. Figure 5a also has the IR spectrum for scorodite
20 and it is clear that formation of scorodite, as has been proposed in some studies,²⁴ does not
21 explain the observed change in shape of the ATRIR spectra as Γ increases.

22 ATRIR spectra were also measured of ferrihydrite pastes obtained by centrifuging suspensions
23 5-15 minutes after AsO_4^{-3} had been added either a) prior to ferrihydrite precipitation (i.e.

1 coprecipitated), b) to ferrihydrite that had been freeze dried and then resuspended in electrolyte
2 or c) to ferrihydrite that had been aged in the electrolyte for 24 h but had not been dried. The
3 three spectra have a maximum at 790 cm^{-1} and a shoulder at $\approx 870\text{ cm}^{-1}$ (Figure 5b). In the
4 coprecipitated system the shoulder is most pronounced and at 875 cm^{-1} in the 2nd derivative while
5 for the freeze dried ferrihydrite the shoulder is less pronounced and at 864 cm^{-1} in the 2nd
6 derivative. The pastes with AsO_4^{-3} sorbed for 5 minutes on a ferrihydrite that had not been dried
7 are intermediate between the coprecipitated and sorbed on freeze dried.

8 The nanometer sized primary ferrihydrite particles are composed of between 20 and 60
9 domains²⁵ and in coprecipitation experiments AsO_4^{-3} can sorb onto domain surfaces prior to
10 aggregation and as the coprecipitates age the process of iron oxide aggregation or crystal growth
11 displaces AsO_4^{-3} causing desorption to occur over time.²³ This has been described as the reverse
12 of “post synthesis” absorption of AsO_4^{-3} where the AsO_4^{-3} has been considered to start at the
13 ferrihydrite particle surface and diffuse to sorption sites located within particles.²³ The spectra in
14 Figure 5 support this model from Fuller et al²³ in which slow diffusion of AsO_4^{-3} from external
15 sorption sites to internal sorption sites accounts for the slow approach to equilibrium. Initially
16 the ATRIR spectra of AsO_4^{-3} in the *in situ* experiments are similar to the spectra where AsO_4^{-3}
17 had just been added to freeze dried ferrihydrite, where AsO_4^{-3} species at the particle surface
18 would dominate. Over time the ATRIR spectra of AsO_4^{-3} in the *in situ* experiments change to
19 become similar to the spectra from the system where AsO_4^{-3} -ferrihydrite had just been
20 coprecipitated, where AsO_4^{-3} species at sites located within particles would be more prevalent. It
21 should be noted that in the case of the *in situ* experiments the ferrihydrite film had been dried
22 onto the ATR crystal.

23 The shift in the ATRIR spectra over time in the *in situ* experiments and the contrast in the
24 spectra for the coprecipitation vs. freeze dried systems described above suggest that the

1 coordination environment of AsO_4^{-3} on an external sorption site is different from AsO_4^{-3} on an
2 internal surface site. It has been proposed that H_4SiO_4 co-precipitated with ferrihydrite may
3 bridge domains^{25, 26} and in the case of AsO_4^{-3} there could also be bridging between particles or
4 domains which could be electrostatic or covalent. It is also noteworthy that when AsO_4^{-3} was
5 exposed for just 5 minutes to ferrihydrite that had not been dried the ATRIR spectrum was
6 intermediate between the spectra for the coprecipitated and sorbed on freeze dried ferrihydrite
7 systems. Comparing this to the shoulder position in the *in situ* spectra on the dried ferrihydrite
8 film suggests that some development of AsO_4^{-3} complexes on internal sorption sites (by diffusion
9 or by bridging particles) is fairly rapid with a ferrihydrite that has not been dried.

10

11 **References**

- 12 1. Smith, A. H.; Lingas, E. O.; Rahmen, M., Contamination of drinking-water by arsenic in
13 Bangladesh: a public health emergency. *Bulletin of The World Health Organization* **2000**, *78*,
14 1093-1103.
- 15 2. Raven, K. P.; Jain, A.; Loeppert, R. H., Arsenite and arsenate adsorption on ferrihydrite:
16 kinetics, equilibrium, and adsorption envelopes. *Environmental Science & Technology* **1998**, *32*,
17 (3), 344-349.
- 18 3. Gustafsson, J. P.; Bhattacharya, P., Geochemical modelling of arsenic adsorption to oxide
19 surfaces. In *Arsenic in soil and groundwater environment. Biogeochemical interactions, health*
20 *effects and remediation.*, Bhattacharya, B.; Mukherjee, A. B.; Bundschuh, J.; Zevenhoven, R.;
21 Loeppert, R. H., Eds. Elsevier: Oxford, 2007.
- 22 4. Ali, M. A.; Dzombak, D. A., Competitive sorption of simple organic acids and sulfate on
23 goethite. *Environmental Science & Technology* **1996**, *30*, (4), 1061-1071.
- 24 5. Dol Hamid, R.; Swedlund, P. J.; Song, Y.; Miskelly, G. M., Ionic strength effects on
25 silicic acid (H_4SiO_4) sorption and oligomerization on an iron oxide surface: an interesting
26 interplay between electrostatic and chemical forces. *Langmuir* **2011**, *27*, (21), 12930-12937.
- 27 6. Swedlund, P. J.; Webster, J. G., Adsorption and polymerisation of silicic acid on
28 ferrihydrite, and its effect on arsenic adsorption. *Water Research* **1999**, *33*, (16), 3413-3422.
- 29 7. Swedlund, P. J.; Webster, J. G.; Miskelly, G. M., Goethite adsorption of Cu(II), Pb(II),
30 Cd(II), and Zn(II) in the presence of sulfate: Properties of the ternary complex. *Geochim.*
31 *Cosmochim. Acta* **2009**, *73*, (6), 1548-1562.
- 32 8. Catalano, J. G.; Park, C.; Fenter, P.; Zhang, Z., Simultaneous inner- and outer-sphere
33 arsenate adsorption on corundum and hematite. *Geochim. Cosmochim. Acta* **2008**, *72*, (8), 1986-
34 2004.

- 1 9. Hiemstra, T.; Van Riemsdijk, W. H., Surface structural ion adsorption modeling of
2 competitive binding of oxyanions by metal (hydr)oxides. *J. Colloid Interface Sci.* **1999**, *210*, (1),
3 182-193.
- 4 10. Scheinost, A. C.; Abend, S.; Pandya, K. I.; Sparks, D. L., Kinetic Controls on Cu and Pb
5 Sorption by Ferrihydrite. *Environmental Science & Technology* **2001**, *35*, (6), 1090-1096.
- 6 11. Zhang, J.; Stanforth, R., Slow adsorption reaction between arsenic species and goethite
7 (α -FeOOH): diffusion or heterogeneous surface reaction control. *Langmuir* **2005**, *21*, (7), 2895-
8 2901.
- 9 12. Connor, P. A.; McQuillan, A. J., Phosphate adsorption onto TiO₂ from aqueous
10 solutions: an in situ internal reflection infrared spectroscopic study. *Langmuir* **1999**, *15*, (8),
11 2916-2921.
- 12 13. Atkinson, R. J.; Hingston, F. J.; Posner, A. M.; Quirk, J. P., Elovich equation for the
13 kinetics of isotopic exchange reactions at solid-liquid interfaces. *Nature* **1970**, *226*, (5241), 148-
14 149.
- 15 14. Tsang, S.; Phu, F.; Baum, M. M.; Poskrebyshev, G. A., Determination of
16 phosphate/arsenate by a modified molybdenum blue method and reduction of arsenate by S₂O₄²⁻.
17 *Talanta* **2007**, *71*, (4), 1560-1568.
- 18 15. Schwertmann, U.; Cornell, R. M., *Iron oxides in the laboratory: preparation and*
19 *characterization*. Wiley-VCH: New York, 1991.
- 20 16. Song, Y. T.; Swedlund, P. J.; McIntosh, G. J.; Cowie, B. C. C.; Waterhouse, G. I. N.;
21 Metson, J. B., The Influence of Surface Structure on H₄SiO₄ Oligomerization on Rutile and
22 Amorphous TiO₂ Surfaces: An ATR-IR and Synchrotron XPS Study. *Langmuir* **2012**, *28*, (49),
23 16890-16899.
- 24 17. Dzombak, D. A.; Morel, F. M. M., *Surface complexation modeling. Hydrous ferric oxide*.
25 John Wiley & Sons, Inc.: New York, 1990.
- 26 18. Westall, J. C. *FITEQL A computer program for determination of chemical equilibrium*
27 *constants from experimental data. Version 2.0*, Department of Chemistry. Oregon State
28 University.: Corvallis, Oregon., 1982.
- 29 19. Kosmulski, M., How to handle the ion adsorption data with variable solid-to-liquid ratios
30 by means of FITEQL. *Colloids and Surfaces a-Physicochemical and Engineering Aspects* **1999**,
31 *149*, (1-3), 397-408.
- 32 20. Herbelin, A.; Westall, J. *FITEQL-A Computer Program for Determination of Chemical*
33 *Equilibrium Constants from Experimental Data. Version 4.0*; Oregon State University, 1999.
- 34 21. Gustafsson, J. P. *Visual MINTEQ Version. 2.61*, Visual MINTEQ Version. 2.61: 2009.
- 35 22. Das, S.; Hendry, M. J.; Essilfie-Dughan, J., Effects of adsorbed arsenate on the rate of
36 transformation of 2-line ferrihydrite at pH 10. *Environmental Science & Technology* **2011**, *45*,
37 (13), 5557-5563.
- 38 23. Fuller, C. C.; Davis, J. A.; Waychunas, G. A., Surface-Chemistry of Ferrihydrite .2.
39 Kinetics of Arsenate Adsorption and Coprecipitation. *Geochim. Cosmochim. Acta* **1993**, *57*, (10),
40 2271-2282.
- 41 24. Muramatsu, C.; Sakata, M.; Mitsunobu, S., Immobilization of Arsenic(V) during the
42 Transformation of Ferrihydrite: A Direct Speciation Study Using Synchrotron-based XAFS
43 Spectroscopy. *Chem. Lett.* **2012**, *41*, (3), 270-271.
- 44 25. Parfitt, R. L.; Gaast, S. J. V. d.; Childs, C. W., A structural model for natural siliceous
45 ferrihydrite. *Clays Clay Miner.* **1992**, *40*, 675-681.

1 26. Swedlund, P. J.; Sivaloganathan, S.; Miskelly, G. M.; Waterhouse, G. I. N., Assessing the
2 role of silicate polymerization on metal oxyhydroxide surfaces using X-ray photoelectron
3 spectroscopy. *Chem. Geol.* **2011**, *285*, (1-4), 62-69.

4

5

6

1 **Table 1** Equilibrium expressions and constants for arsenate surface complexation reactions.

2

<i>Equilibrium Expression^a</i>	<i>logK_{As}^b</i>	<i>Range</i>	<i>Slope^c</i>
$(\equiv \text{FeH}_2\text{AsO}_4) = (\equiv \text{FeOH})(\text{AsO}_4^{-3})(\text{H}^+)^3 K_{\text{As1}}$	31.0 (30.5, 31.5)	30.2-32.5 ^d	0.54 (-0.03, 1.1)
$(\equiv \text{FeHASO}_4^{-1}) = (\equiv \text{FeOH})(\text{AsO}_4^{-3})(\text{H}^+)^2 e^{\frac{F\Psi}{RT}} K_{\text{As2}}$	25.8 (25.6, 26.1)	25.0-27.0 ^d	0.47 (0.06, 0.87)
$(\equiv \text{FeAsO}_4^{-2}) = (\equiv \text{FeOH})(\text{AsO}_4^{-3})(\text{H}^+) e^{\frac{2F\Psi}{RT}} K_{\text{As3}}$	19.5 (19.4, 19.6)	19.8-20.3 ^d	0.18 (-0.3, 0.6)
$(\equiv \text{FeOHAsO}_4^{-3}) = (\equiv \text{FeOH})(\text{AsO}_4^{-3}) e^{\frac{3F\Psi}{RT}} K_{\text{As4}}$	11.9 (11.9, 12.0)	10.9-12.8 ^e	0.0 (-0.4, 0.4)

3 ^a F, Ψ, R, T have their usual meaning, (X)=activity of species X

4 ^b Weighted average with 95 % confidence interval in brackets (data from ³)

5 ^c Slope and 95 % confidence interval for $\log K_{\text{Asn}} = m(\log(t)) + c$ where t is reaction time (data from ³)

6 ^d Highest value derived from Swedlund and Webster data ⁶

7 ^e Swedlund and Webster $\log K_{\text{As4}}$ values were 11.40-11.73 ⁶

8

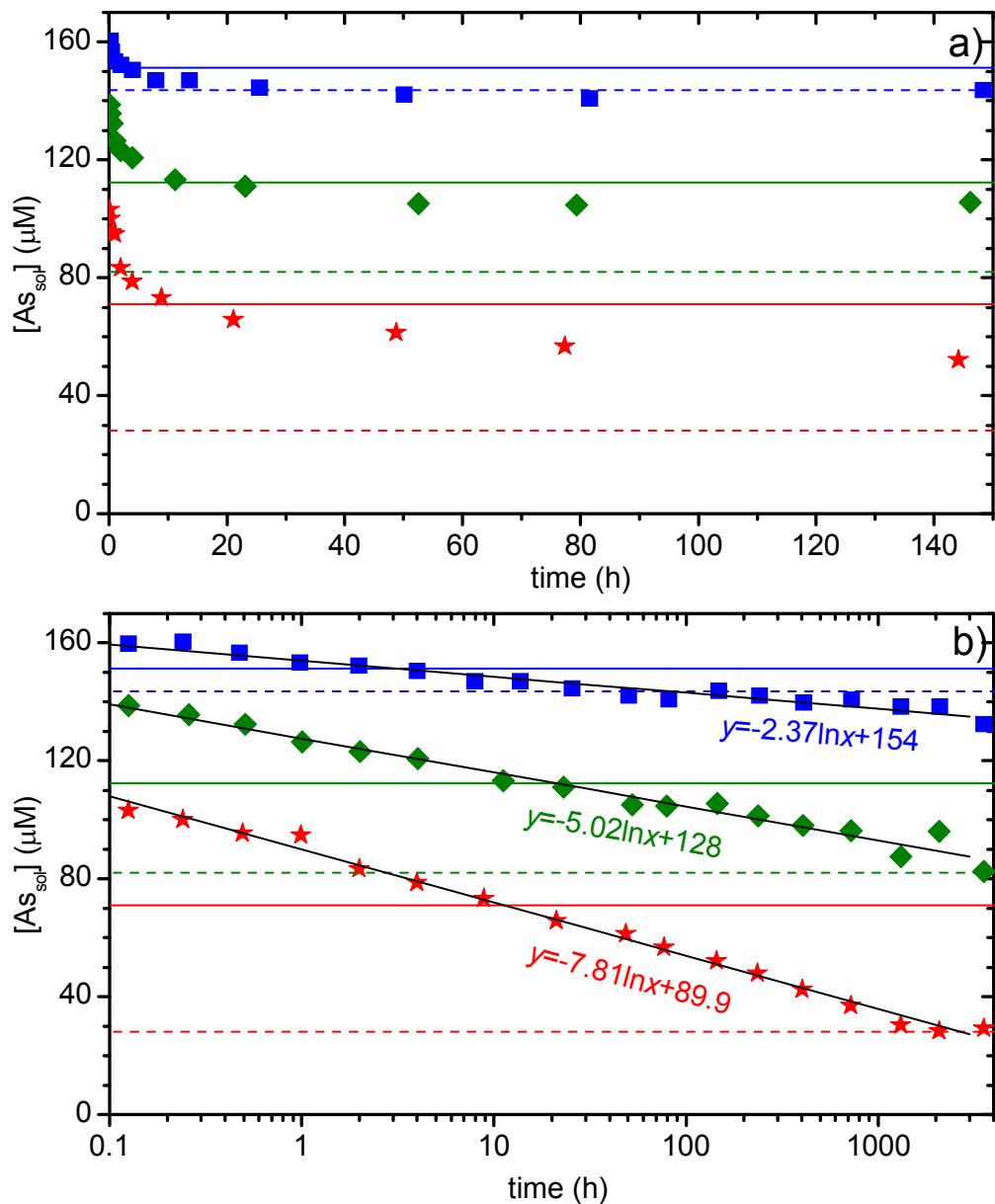
1
2
3
4

Table 2 The log equilibrium constants ($\log K_{Asn}$) values and associated standard deviations for arsenate adsorption to ferrihydrite calculated FITEQL4 which take into account adsorption time. The $As_T \approx 50 \mu M$ pH 6 values were excluded from the FITEQL4 input file.

Hours	$\log K_{As4}$	σ_4	$\log K_{As3}$	σ_3	$\log K_{As2}$	σ_2	$\log K_{As1}$	σ_1	WSOS/DF
0.5	12.135	0.069	19.202	0.105	25.569	0.103	30.049	0.309	2.026
1	12.205	0.075	19.381	0.098	25.724	0.096	30.405	0.168	1.683
2	12.293	0.055	19.498	0.485	25.891	0.096	30.660	0.111	1.416
4	12.404	0.079	19.565	0.107	26.064	0.075	30.889	0.093	1.292
8	12.540	0.080	19.576	0.138	26.236	0.065	31.120	0.080	1.607
12	12.597	0.077	19.646	0.124	26.315	0.062	31.238	0.074	1.779
24	12.650	0.081	19.745	0.119	26.432	0.058	31.418	0.068	1.748
48	12.699	0.086	19.838	0.114	26.548	0.055	31.589	0.064	1.700
96	12.743	0.090	19.927	0.109	26.663	0.054	31.758	0.062	1.627
150	12.769	0.094	19.983	0.107	26.736	0.053	31.866	0.062	1.555
300	12.808	0.100	20.062	0.103	26.851	0.052	32.035	0.062	1.473
600	12.844	0.107	20.137	0.101	26.967	0.051	32.206	0.062	1.392
1000	12.869	0.107	20.186	0.101	27.054	0.051	32.334	0.062	1.400
1300	12.883	0.114	20.209	0.100	27.100	0.052	32.400	0.064	1.442

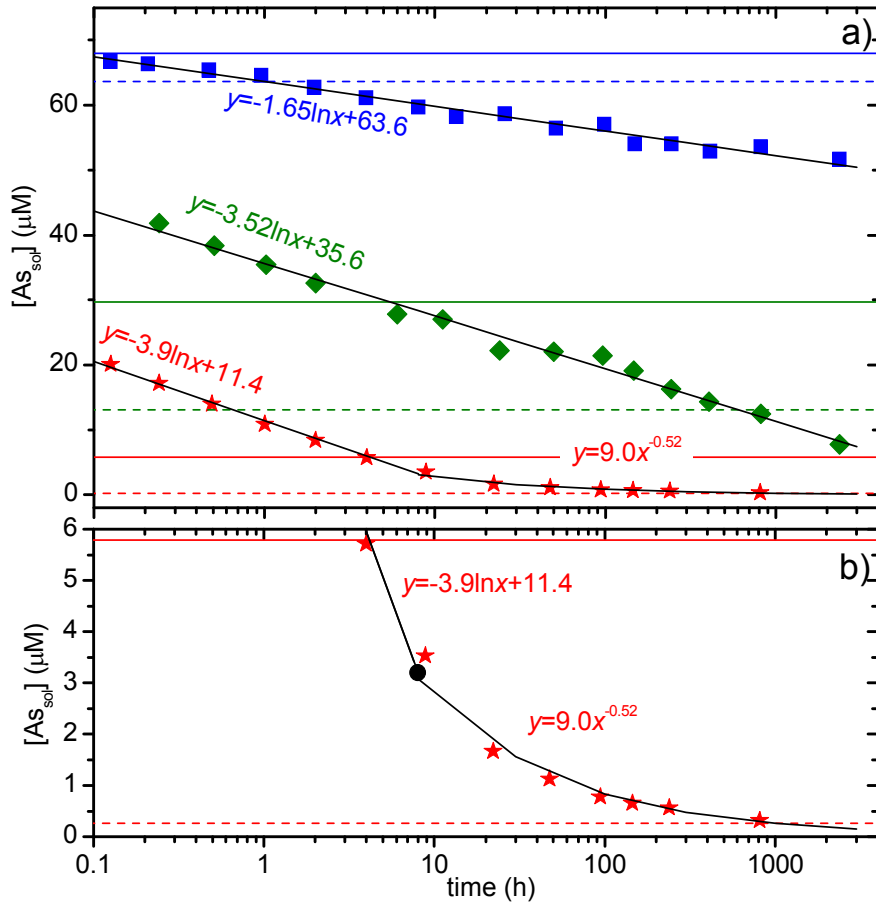
5
6

1

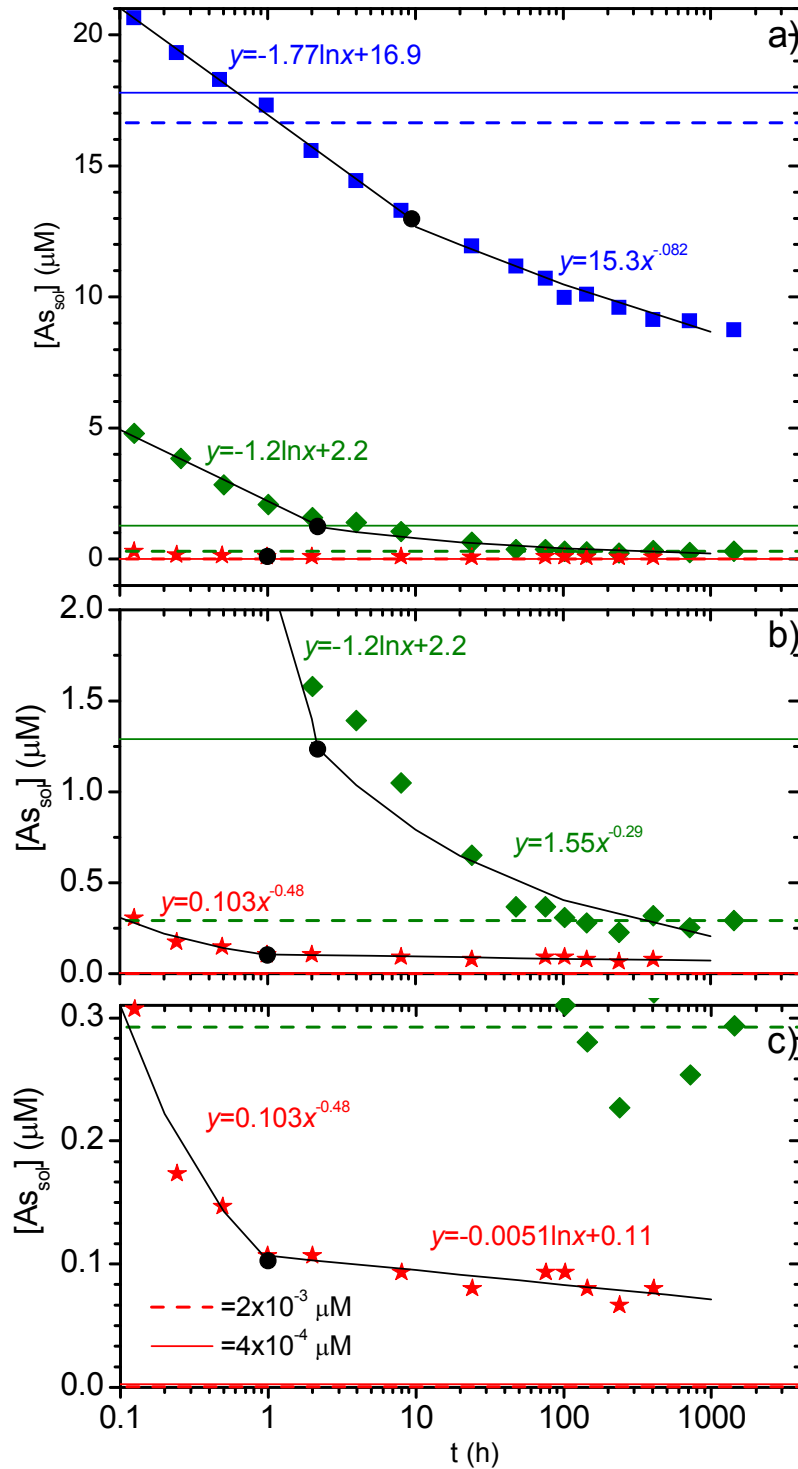


2 **Figure 1** Solution arsenate concentrations over time in systems with ≈ 1 mM Fe, 200 μM total $[AsO_4^{3-}]$ and
 3 0.06 M $NaNO_3$. Blue, green and red are pH 10, 8 and 6 respectively. Horizontal lines are the model
 4 predictions using the values from Gustafsson²¹ (solid lines) and Swedlund and Webster⁶ (dashed lines).

5

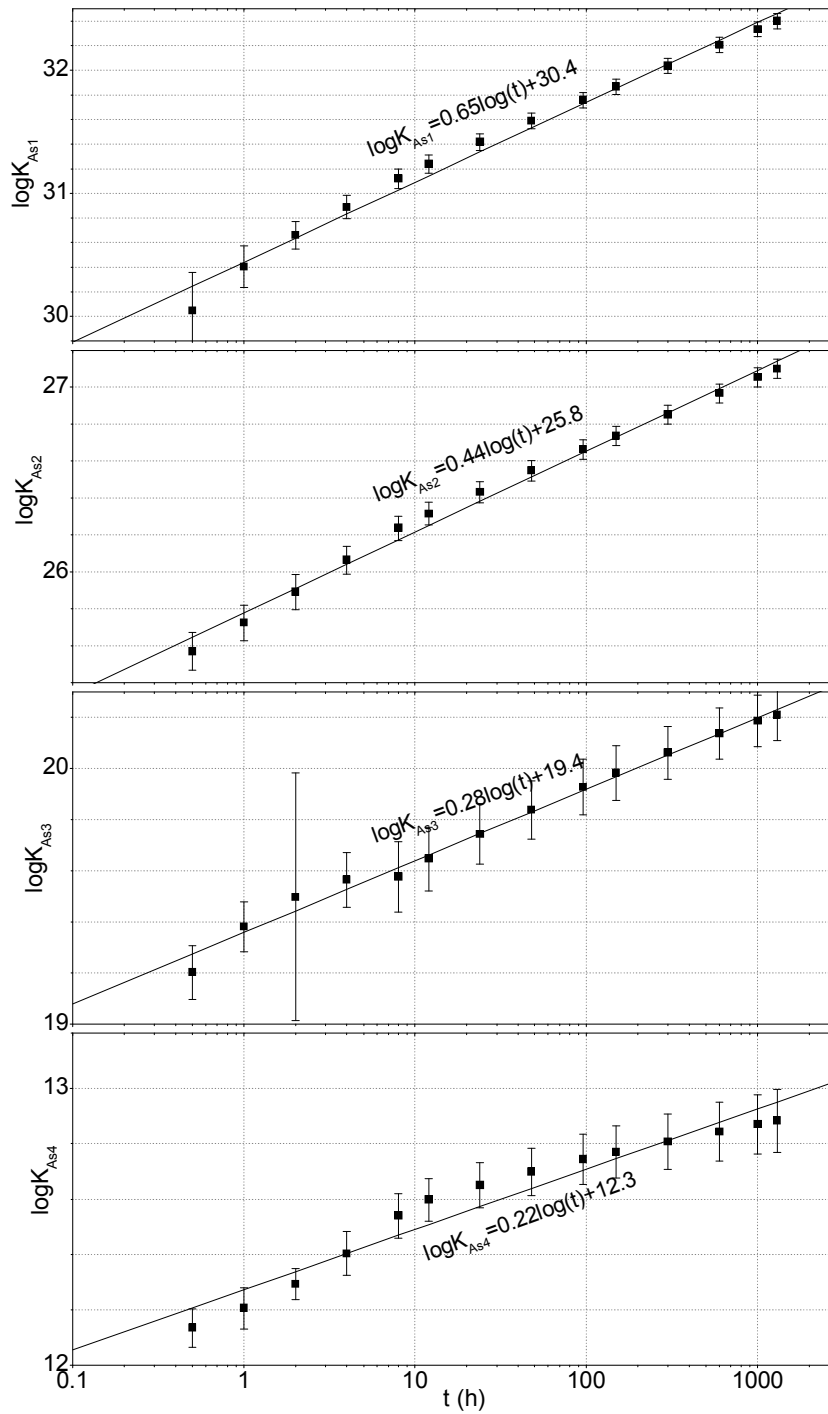


1 **Figure 2** Solution arsenate concentrations over time in systems with ≈ 1 mM Fe, 100 μM total $[AsO_4^{-3}]$ and
 2 0.06 M $NaNO_3$. Blue, green and red are pH 10, 8 and 6 respectively. Horizontal lines are the model
 3 predictions using the values from Gustafsson²¹ (solid lines) and Swedlund and Webster⁶ (dashed lines).

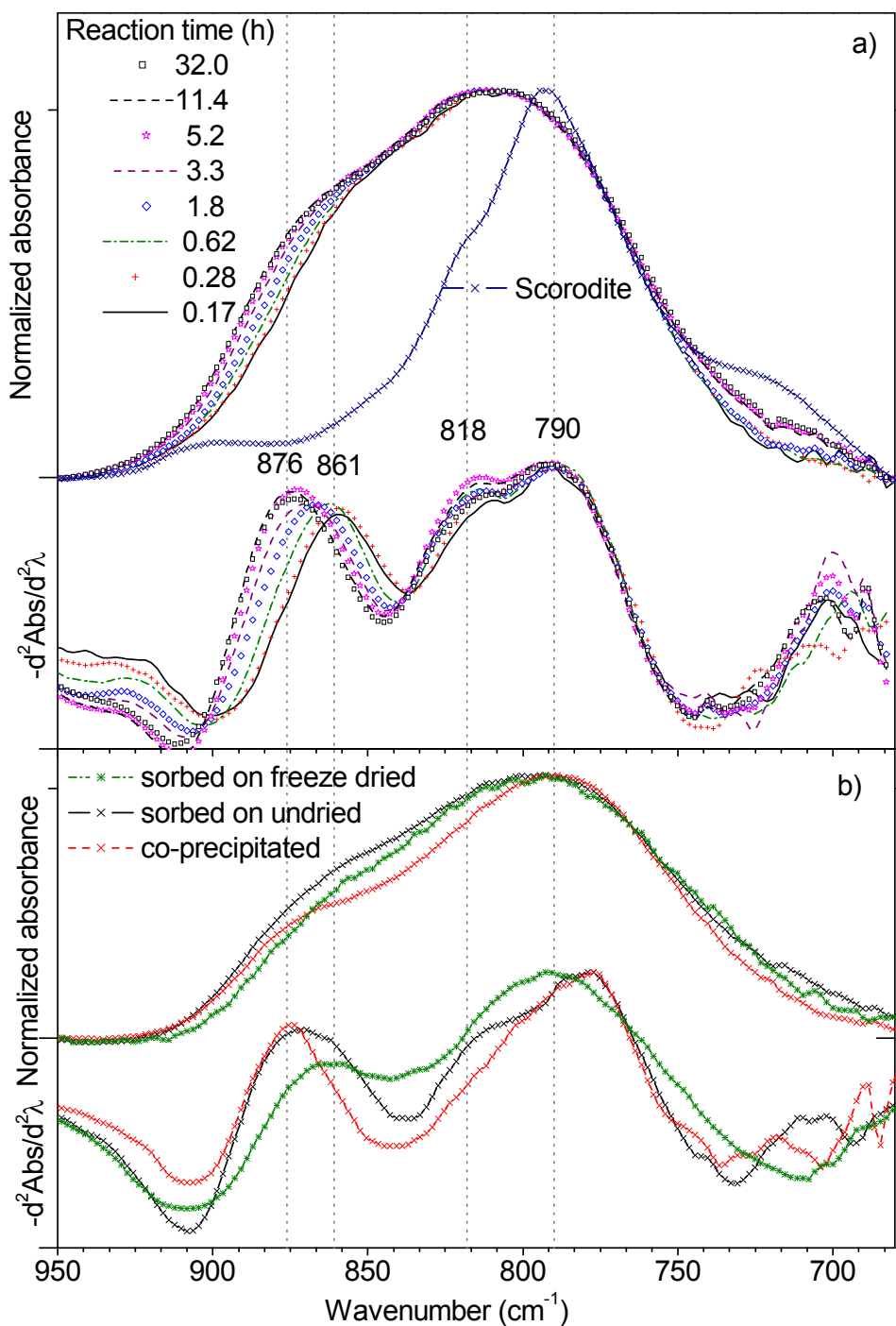


1

2 **Figure 3** Solution arsenate concentrations over time in systems with ≈ 1 mM Fe, $50 \mu M$ total $[AsO_4^{-3}]$ and
 3 0.06 M $NaNO_3$. Blue, green and red are pH 10, 8 and 6 respectively. Horizontal lines are the model
 4 predictions using the values from Gustafsson²¹ (solid lines) and Swedlund and Webster⁶ (dashed lines).



1 **Figure 4** Optimized $\log K$ values from the data in Figures 1-3. Error bars are the reported standard
 2 deviations in $\log K$.
 3



1
 2 **Figure 5** Absorbance normalized ATR-IR spectra and the negative 2nd derivatives of AsO_4^{3-} on
 3 ferrihydrite in systems with 200 μM total AsO_4^{3-} at pH 8 and 0.06 M NaCl a) *in situ* spectra recorded over
 4 time as AsO_4^{3-} reacted with a ferrihydrite film dried onto an ATRIR crystal b) spectra of pastes obtained by
 5 centrifugation 5-10 minutes after AsO_4^{3-} was added to ferrihydrite or was coprecipitated with ferrihydrite.
 6 The IR spectrum of scorodite is also shown.